Chemistry–A European Journal
Research Article
doi.org/10.1002/chem.202403679
Chemistry Europe
European Chemical Societies Publishing
www.chemeurj.org

Phenazinium- and Malachite Green-Based Pd(II) Cages: Chiroptical Discrimination of Nucleoside Triphosphates

Armin Durmisevic,[a] Irene Regeni,[b] Mark Ely Namoro,[a] Ananya Baksi,[c] and Guido H. Clever*[a]

Organic chromophores have been successfully implemented into supramolecular systems to bestow them with distinct photophysical properties for various applications, ranging from solar energy conversion, photochemical reactions or as receptors for guest molecules with optical readout. We had previously introduced first members of the large family of coal-tar dyes (methylene blue, crystal violet and rhodamine) as integral components of coordination cages. Here, we add two new chromophores, malachite green (**MGP**) and a purple phenazinium dye (**PHP**), serving as backbones of bis-monodentate banana-shaped ligands with pyridine donors. We show the formation of corresponding green and purple coloured Pd_2L_4 coordination cages and investigate their interaction with chiral guest molecules via UV-Vis and CD spectroscopy. The **PHP** cage can be used to recognize nucleoside triphosphates, based on chirality transfer from the guests to the structurally flexible helicate. In combination with the already known methylene blue cage **MBP** we could further differentiate between all four canonical NTPs through characteristic changes in the observed CD signatures.

Introduction

Supramolecular architectures have been extensively used as scaffolds for bringing together functionalities in a defined arrangement. In particular, various organic chromophores were integrated, e.g. porphyrins as light harvesting units to mimic solar energy conversion,[1–3] and chiral compounds with strong absorptive or emissive properties for various applications such as light sources, displays or catalysis.[4–7] Additionally, the use of such chromophore assemblies has been explored in a biological context for the imagining of tissue and cells or in photodynamic therapy.[8–13]

In coordination cages, spontaneously assembling from a defined number of organic ligands through coordination of a transition metal cation such as Pd^{2+}, several different chromophores have been integrated to date.[14] Giving (chir)optical properties to such systems allows to employ them for sensing[15] and energy transfer[16,17] applications. It can also serve to optically monitor chemical transformations.[18–20] Many of the so far incorporated chromophores, however, show their major absorption characteristics in the UV to short-wavelength region with only faint absorption in the visible range. This can hamper perception by the naked eye and lead to strong spectral overlap between the chromophore and other structural moieties, causing unwanted interference such as intra-assembly dissipation of electronic excitation. Implementing well-known organic dyes that show strong absorption in the visible region into ligand backbones can separate absorption features of the dye-based ligands from other components such as guest molecules.[21–26] Recently, we and others[27,28] started to introduce various established chromophores as integral structural components into Pd-based coordination cages, among them blue/green coloured azulenes,[29] different derivatives of the "Ferrari Red"-nicknamed diketopyrrolopyrroles[30] and – with Lützen *et al.* – a BODIPY.[31] In all cases, absorption properties of the parental dyes could be transferred to the supramolecular assembly. In addition, we showed how some of the coal-tar dyes,[32–35] amongst the first commercial products from large scale chemical industry in the 19th century, can be implemented into the backbones of pyridine- and isoquinoline-based bridging ligands without compromising their colour-giving auxochromic features.[36] While the corresponding, strongly coloured coordination cages showed first promising results concerning the chiroptical readout of their interaction with a variety of chiral guests, their potential application in selective sensing or analyte differentiation has not yet been investigated. In this work we introduce two new coal tar dye-based cages based on malachite green (**MGP**) and a purple phenazinium dye (**PHP**), thereby complementing the "rainbow" of coloured assemblies developed in our lab. We further show how the combination of two dye-based cages can be utilized to differentiate all four canonical ribonucleoside triphosphates in a single system based on CD measurements.[21,37–43]

[a] *A. Durmisevic, M. E. Namoro, G. H. Clever*
Department of Chemistry and Chemical Biology, TU Dortmund University, Otto-Hahn-Str. 6, 44227 Dortmund, Germany
E-mail: guido.clever@tu-dortmund.de

[b] *I. Regeni*
Leiden Institute of Chemistry, Leiden University, 2333CC Leiden, The Netherlands

[c] *A. Baksi*
Department of Chemistry, Jadavpur University, Kolkata, West Bengal 700032, India

Supporting information for this article is available on the WWW under https://doi.org/10.1002/chem.202403679

Results and Discussion

First, we introduced a purple *N*-ethyl phenazinium chromophore and the malachite green dye into the molecular structure of two new cationic, bis-monodentate ligands (**PHP** and **MGP**). Instead of often employed alkynyl or phenylene linkers, we connected the pyridyl donor moieties via piperazine linkers to allow keeping the dialkyl amino auxochromic substituents on the chromophore π-systems.[36] We then investigated the formation of homoleptic Pd_2L_4 cages and their host–guest complexes, with a focus on the interaction of Pd_2(**PHP**)$_4$ as well as previously reported methylene blue-based cage Pd_2(**MBP**)$_4$ with ribonucleoside triphosphates (NTP). Sequential titration experiments, first using the two individual cages and then a narcissistically self-sorted mixture of both, with the NTPs were followed by circular dichroism (CD) spectroscopy.

The synthetic route towards ligand **PHP** starts from phenazine, on which a single *N*-alkylation was selectively performed through the use of triethyl oxonium tetrafluoroborate. Subsequent introduction of two 1-(pyridin-3-yl)piperazine moieties was achieved in a regioselective manner (*meta* to the alkylated nitrogen) via oxidative coupling using molecular oxygen to yield the target compound as a dark violet solid. Ligand **MGP** was achieved through a Grignard reaction of phenylmagnesium bromide with previously synthesized Michler's ketone ligand **MKP** followed by acidic workup with HBF_4 to obtain the product as a green precipitate. The strategic selection of piperazines as aliphatic linkers between the backbone and donor moieties was imperative to maintain the structural integrity of the parental dyes and their electronic properties (Figure 1).[36] Formation of both cages Pd_2(**PHP**)$_4$ as well as Pd_2(**MGP**)$_4$ was achieved in DMSO-d_6 and DMF-d_7, respectively, by heating a 2:1 mixture of ligand and palladium source $[Pd(CH_3CN)_4](BF_4)_2$ at 70 °C for 15 min. In accordance with previously reported Pd(II) cages, a downfield shifting of the pyridine proton signals in the ^{1}H-NMR spectra could be observed.[44] The formation of both coordination cages was further confirmed through ^{1}H-DOSY NMR measurements, indicating an approximate doubling of the hydrodynamic radii from the free ligands to the respective cages (Figures 2a and SI). Interestingly, although ligand **MGP** was fully soluble in DMSO-d_6, decolourization of the solution proceeded quickly resulting in a faintly yellow colour and no clean cage formation could be achieved from this solution. This is likely due to the formation of the leuco-malachite green form, either through a nucleophilic attack of water, solvent DMSO or an anion to the central carbocation (even facilitated in the cationic Pd cage by an increase in electrophilic character of the dye) or through its reduction to a triaryl methane. The same cage formed in DMF showed a higher stability over time. When adding small amounts of water to the DMSO or DMF solution of ligand **MGP** or cage Pd_2(**MGP**)$_4$, however, it deteriorated quickly as judged by NMR analysis and lost its colour, forming an insoluble precipitate.

High-resolution ESI mass spectrometry (HR-ESI-MS) measurements confirmed the 2:1 stoichiometry of ligand to Pd(II) with prominent signals corresponding to differently charged species for BF_4^- adducts of cage Pd_2(**PHP**)$_4$ (Figure 2b). Due to the instability of cage Pd_2(**MGP**)$_4$, no mass spectra could be recorded to fully confirm the stoichiometry of this assembly. We then wanted to compare the host capabilities of these newly established dye-based cages concerning their interaction with chiral nucleoside triphosphates ATP, GTP, CTP and UTP, added as their tri-sodium salts. All guests were dissolved in D_2O and added to the individual cage solutions in DMSO and DMF. Again, we noticed a rapid decolourization of the **MGP**-based cage after adding even small amounts of aqueous guest solution, concomitant with an onset of precipitation. This rendered the whole **MGP** system unviable for further inves-

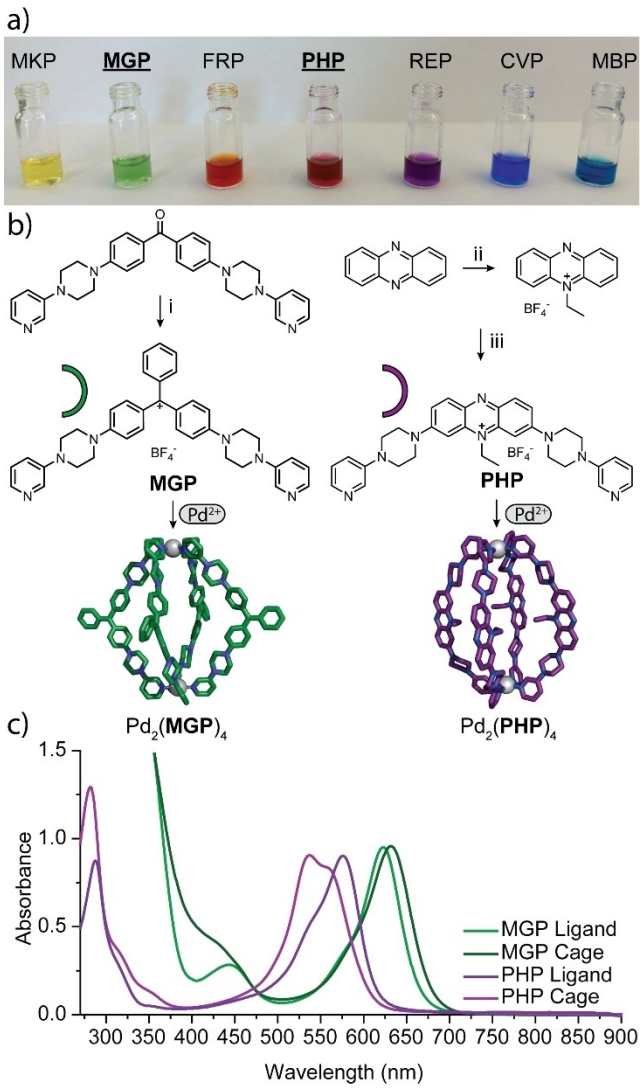

Figure 1. a) Rainbow of dye-based ligands from left to right: Michler's ketone (**MKP**),[36] malachite green (**MGP**, this work), diketopyrrolopyrrole ('Ferrari Red', **FRP**),[30] phenazinium (**PHP**, this work), rhodamine ester (**REP**),[36] crystal violet (**CVP**)[36] and methylene blue (**MBP**).[36] b) Synthetic routes towards malachite green and phenazinium ligands **MGP** and **PHP**: i) PhMgBr in dry THF, 5 min reflux, then to r.t. followed by slow addition of HBF_4; ii) OEt_3BF_4 in dichloromethane, 24 h, r.t.; iii) 3-(piperazin-3-yl)pyridine or 8-(piperazin-1-yl)isoquinoline in ethanol, 78 °C, O_2, 96 h. c) UV-Vis spectra of dye-based ligands and cages in DMSO and DMF at equal chromophore concentration (0.7 mM).

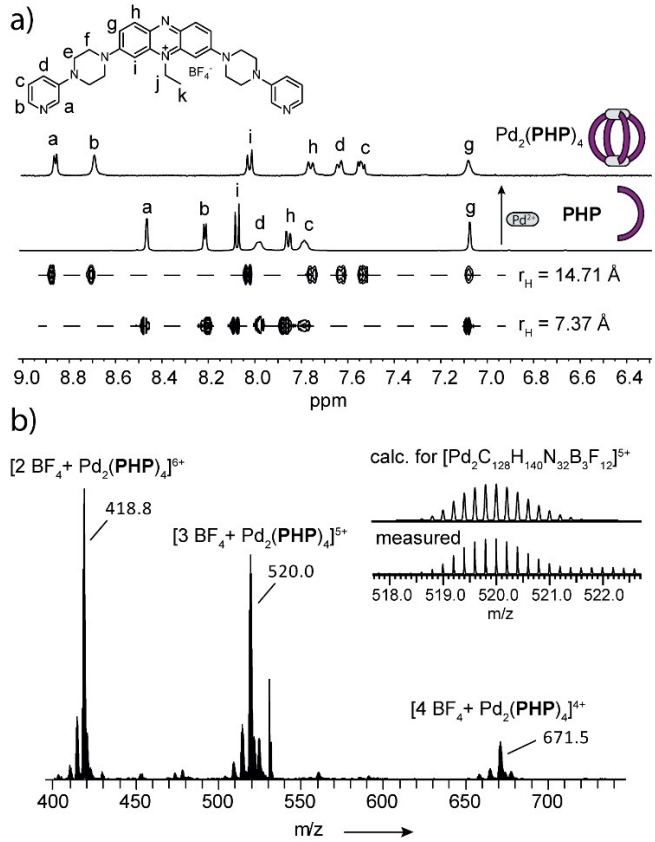

Figure 2. a) ^{1}H and ^{1}H-DOSY NMR spectra of ligand **PHP** and cage Pd_2(**PHP**)$_4$ in DMSO-d_6 at 298 K. b) HR-ESI-MS spectrum of Pd_2(**PHP**)$_4$.

tigations. We therefore continued with the more stable Pd_2(**PHP**)$_4$ cage and investigated the host–guest interactions by means of CD and UV-Vis spectroscopy. The recorded CD spectra indicated that the highly positively charged (8+) Pd_2(**PHP**)$_4$ cage showed preferential interaction with negatively charged (3−) ribonucleoside triphosphates (SI). We observed that the guanosine triphosphate (GTP) lead to induction of a significant CD signal coinciding with the absorption region of the **PHP** cage. We then expanded the selection to ATP, CTP and UTP and indeed confirmed that all showed host–guest interactions resulting in an induced circular dichroism signal (ICD, Figure S24). Upon further titration with these guests, an interesting difference in the concentration dependence of the ICD signal was discovered. If less than one equivalent of GTP compared to cage was present, a positive Cotton effect on the longest wavelength absorption of the host–guest complex could be detected. Higher amounts of GTP lead to a band inversion and to a negative Cotton effect in that region. All other nucleotides showed a positive Cotton effect, indifferent to the ratio between cage and guest. We assume that the addition of one equivalent of GTP saturates the host's inner void, leading the host–guest complex to adopt a defined helical conformation as a function of the guest's chirality. Addition of more GTP then leads to an outside association mode that pushes the conformational equilibrium of the helically chiral host in the opposite direction. While the other NTPs all bind (in)to the cage, they do not seem to show the second effect upon increasing their concentration. With this peculiar behavior, GTP became clearly distinguishable from the other nucleotides by employing cage Pd_2(**PHP**)$_4$ as a sensor. In order to be able to differentiate all four canonical ribonucleotides from each other, a second discrimination step was needed (Figure 3). Using the structurally similar cage Pd_2(**MBP**)$_4$, we investigated its titration-induced chirality changes in presence of all four nucleotides, separately. Contrary to the results obtained with Pd_2(**PHP**)$_4$, now only ATP and CTP showed concentration-dependent Cotton effect switching, thus showcasing a different selectivity of the **MBP**-based cage. The other NTPs did not exhibit a Cotton effect inversion with Pd_2(**MBP**)$_4$ making them thus easily distinguishable from ATP and CTP. Interestingly, when comparing the CD spectra of the two cages after addition of UTP, opposite Cotton effects could be observed (Figure S25). Also cages based on chromophores **CVP** and **REP** were tested in these experiments. While they show emergence of an ICD signal in all cases, no sign switching was observed. In summary, the sequential interaction of individual NTPs with the two individual dye-based cages Pd_2(**PHP**)$_4$ and Pd_2(**MBP**)$_4$ followed by CD, made it possible to either directly identify GTP or UTP from an unknown nucleotide solution or assess if either ATP or CTP are present (Figure 3). A full differentiation of all four nucleotides, however, was not possible with this first approach.

By comparing the absorption differences of the two dye-based cages Pd_2(**PHP**)$_4$ and Pd_2(**MBP**)$_4$ in the visible region, we envisioned that the combination of both in a single titration experiment could lead to a distinguishable CD behaviour for the guests ATP and CTP. The combination of both cages in a 1:1 ratio was first followed by ^{1}H-NMR spectroscopy. Upon immediate mixing of their DMSO solutions, both cages remain intact and do not exchange ligands spontaneously (towards formation of a statistical mixture), as the chemical shifts of the individual cages do not shift and no new signals, indicative of new species, are observed. This holds true even for periods of up to 24 h at room temperature. Although both ligands are of almost identical shape, size and charge, clean narcissistic self-sorting could be observed under these conditions. This feature made it thus possible to exploit the individual interactions of the cages with the nucleotide guests for chiroptical sensing in a single experiment per guest. Only when heating the solution over a prolonged period of time of 24 h at 70 °C a change in the ^{1}H-NMR spectrum can be observed, indicating the formation of a mixture of species as well as the partial release of the **PHP** ligand. Upon titration of CTP and ATP into a mixture of the two cleanly sorted cages, different CD characteristics could be observed. The CD bands after addition of CTP showed no change in sign with increasing guest concentration. Addition of increasing amounts of ATP, however, led to a distinct change in shape of the CD signature with varying host:guest ratio. Most notable is the change of the CD band at 680 nm which changes sign from negative to positive. To note is also the difference in intensity of the CD response in the visible region between the two nucleotides (Figure 4). Thus, by applying a three-step process, which consists of a titration of the unknown guest into a cage solution of Pd_2(**PHP**)$_4$, then separately into a solution of

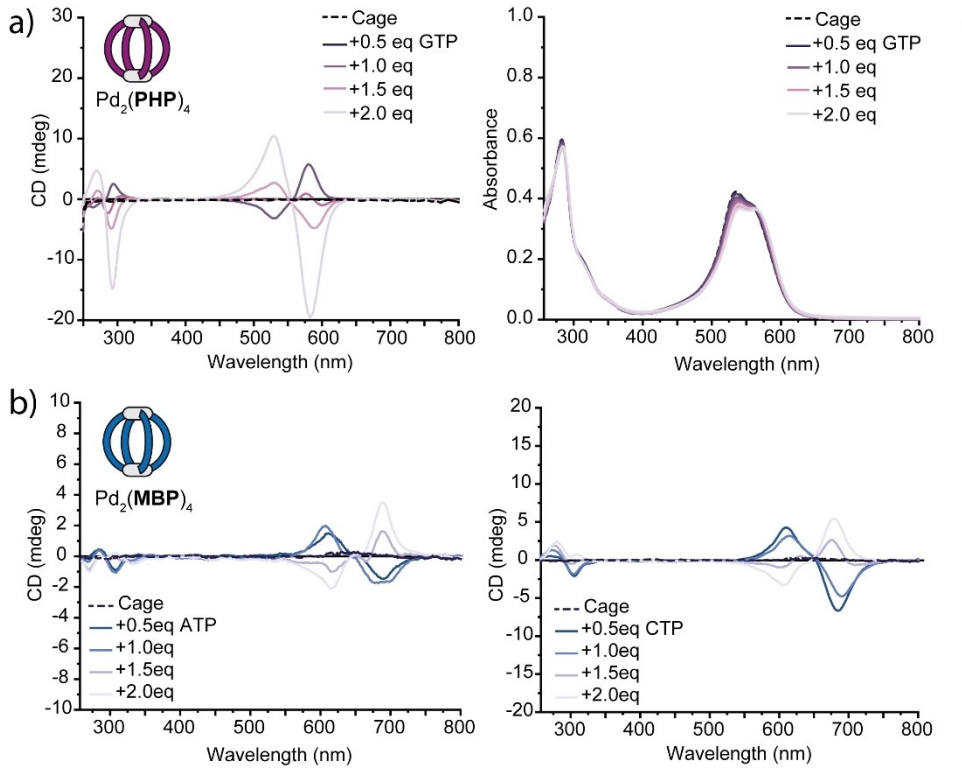

Figure 3. a) Titration of Pd_2(**PHP**)$_4$ with GTP yields an induced circular dichroism (ICD) signal. The Cotton effect on the cage absorptions switches sign after addition of approx. one equivalent of guest. The UV-Vis spectra following the titration of cage Pd_2(**PHP**)$_4$ with GTP showed no drastic changes apart from a slight decrease in signal intensity. b) Titration of Pd_2(**MBP**)$_4$ with nucleoside triphosphates ATP and CTP also showed an inversion of the Cotton effect from positive to negative with increasing nucleotide concentration. Contrary to phenazinium cage Pd_2(**PHP**)$_4$, however, no switching was observed in presence of GTP. c) Table showing if a change of the ICD signal with varying host:guest ratio occurs or not for all four tested dye-based cages. Although **CVP** and **REP** show an ICD signal (see SI), no change of sign could be observed in any case. Total cage concentration was 25 uM in DMSO. The nucleoside triphosphates were dissolved in deionized water.

Pd_2(**MBP**)$_4$ and ultimately into a solution of a 1:1 mixture between the two cages, it is possible to differentiate between all four (A, G, C and U) ribonucleoside triphosphates in solution. Furthermore, it was possible to leverage the mixture of the two cages for the direct differentiation of the single nucleotides by their unique changes in the CD signature dependent on their ratio to the cage.

Additionally, the possibility of differentiating multiple nucleotides simultaneously was investigated. Again, using the 1:1 mixture of Pd_2(**PHP**)$_4$ and Pd_2(**MBP**)$_4$ we can uniquely identify four out of six pairs of ribonucleotides based on their distinctive circular dichroism signature, where only G + C and A + G showed very similar CD signatures throughout the titrations (Figures S30–S32). Notably, when three guest molecules were concurrently introduced, differences emerged solely between combinations inclusive or exclusive of GTP. This observation suggests a discernible preference for GTP interaction exhibited by either cage (Figures S33 and S34). Consequently, the cages may adopt concentration-dependent distinct chiral conformations to optimise interactions with the increase in guest molecule amount interacting with it. However, full verification of this claim was not possible as cryo-HR-ESI-MS measurements only revealed a 1:1 stoichiometry between hosts Pd_2(**PHP**)$_4$ and Pd_2(**MBP**)$_4$ and guests GTP and ATP, respectively. Through trapped ion-mobility measurements coupled to ESI-TOF mass spectrometry (timsTOF), the experimental collisional cross sections (CCS) could be obtained of both empty host and host–guest complex for either cage. The relatively large difference of approx. 25 Å^2 (with the host–guest complex being larger than the free host) indicated that in fact already the first binding nucleotide is not fully engulfed by the cage cavity but at least protrudes partially outside (Figure S29).

Conclusions

We synthesized two novel coal-tar dye-based Pd_2L_4 coordination cages, one based on a purple phenazinium chromophore **PHP** and one based on the malachite green dye **MGP**, both showing strong absorption properties at different wavelengths of the visible spectrum. Due to its chemical fragility, **MGP** could not be used for the subsequent studies with aqueous solutions of chiral nucleoside triphosphates. We were, however, successful in applying the **PHP**-based cage as a supramolecular sensor for the four canonical ribonucleoside triphosphates. The formation of chiral host–guest complexes and the inherent chirality transfer from the NTPs to the flexible host made it possible to use CD spectroscopy as a simple optical readout for the differentiation of the four investigated nucleotides GTP, ATP, CTP and UTP, when combined with a second dye-based

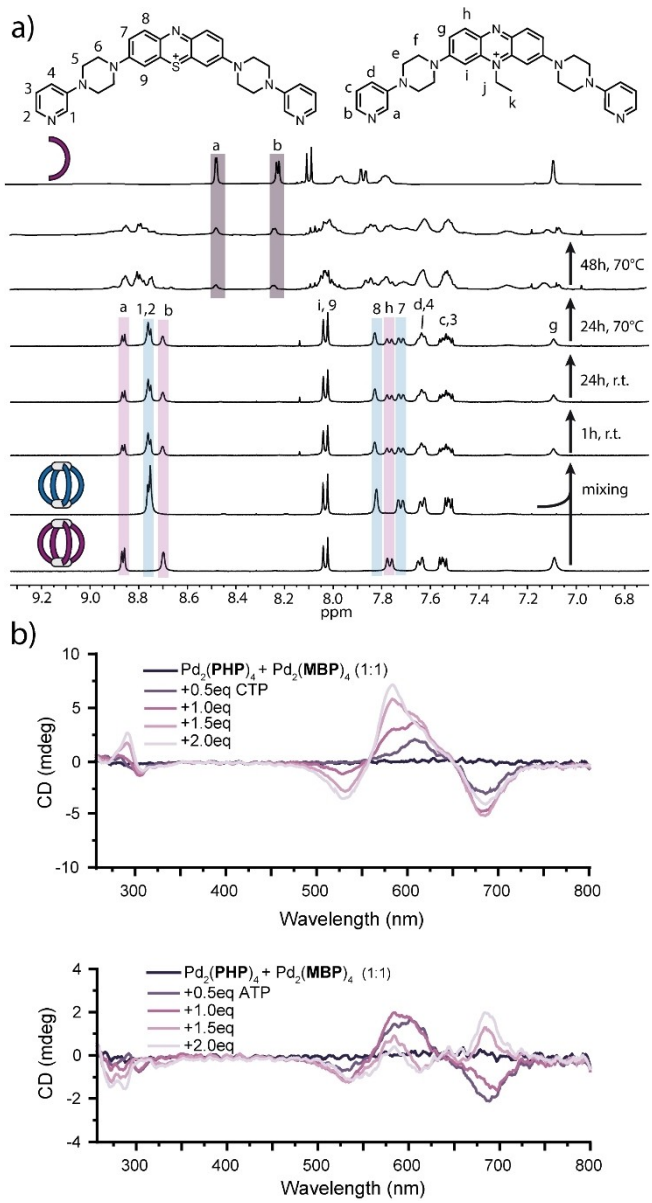

Figure 4. a) ^{1}H-NMR spectra of 1 : 1 mixtures of cages Pd_2(**PHP**)$_4$ and Pd_2(**MBP**)$_4$ in DMSO-d_6 at 298 K. No mixing of ligands occurred within a timeframe of 24 h, indicating a narcissistic self-sorting of the two cages. b) Titration of CTP and ATP guests into a 1 : 1 mixture of cages Pd_2(**PHP**)$_4$ and Pd_2(**MBP**)$_4$. Only ATP showed a concentration-dependent change of the CD signature of the host-guest complex.

cage comprising methylene blue-based ligand **MBP**. Owing to the narcissistic self-sorting of the phenazinium and methylene blue cages, their different absorption properties and chiroptical responses to the NTPs could be employed even in mixture. This new receptor family may find application in the monitoring of complex biological or biomimetic systems, where production or consumption of NTPs at low concentrations can then be easily followed.

Acknowledgements

This work was financed by the Deutsche Forschungsgemeinschaft (DFG, German Research Foundation) under Germany's Excellence Strategy EXC2033, project number 390677874 ("RESOLV"). I.R. thanks the Fonds der Chemischen Industrie (FCI) for a Kekulé PhD fellowship. Open Access funding enabled and organized by Projekt DEAL.

Conflict of Interests

The authors declare no conflict of interest.

Data Availability Statement

The data that support the findings of this study are available from the corresponding author upon reasonable request.

Keywords: Cages · Receptors · Dyes · Phosphates · Host–guest

[1] J. Otsuki, *J. Mater. Chem. A* **2018**, *6*, 6710–6753.
[2] A. Prodi, C. Chiorboli, F. Scandola, E. Iengo, E. Alessio, R. Dobrawa, F. Würthner, *J. Am. Chem. Soc.* **2005**, *127*, 1454–1462.
[3] S. Durot, J. Taesch, V. Heitz, *Chem. Rev.* **2014**, *114*, 8542–8578.
[4] X. Lou, Y. Yang, *Adv. Opt. Mater.* **2018**, *6*, 1800668.
[5] D. Li, J. Wang, X. Ma, *Adv. Opt. Mater.* **2018**, *6*, 1800273.
[6] T. Uchikura, M. Oshima, M. Kawasaki, K. Takahashi, N. Iwasawa, *Angew. Chem. Int. Ed.* **2020**, *59*, 7403–7408.
[7] R. Cibulka, R. Vasold, B. König, *Chem. Eur. J.* **2004**, *10*, 6223–6231.
[8] N. Mehwish, X. Dou, Y. Zhao, C.-L. Feng, *Mater. Horizons* **2018**, *6*, 14–44.
[9] S. Gnaim, A. Scomparin, A. Eldar-Boock, C. R. Bauer, R. Satchi-Fainaro, D. Shabat, *Chem. Sci.* **2019**, *10*, 2945–2955.
[10] S. S. Liow, H. Zhou, S. Sugiarto, S. Guo, M. L. S. Chalasani, N. K. Verma, J. Xu, X. J. Loh, *Biomacromolecules* **2017**, *18*, 886–897.
[11] X. Li, S. Lee, J. Yoon, *Chem. Soc. Rev.* **2018**, *47*, 1174–1188.
[12] R. Chang, E. Nikoloudakis, Q. Zou, A. Mitraki, A. G. Coutsolelos, X. Yan, *ACS Appl. Bio. Mater.* **2019**, *3*, 2–9.
[13] H.-B. Cheng, Y. Cui, R. Wang, N. Kwon, J. Yoon, *Coord. Chem. Rev.* **2019**, *392*, 237–254.
[14] Y. Jiao, Y. Zuo, H. Yang, X. Gao, C. Duan, *Coord. Chem. Rev.* **2021**, *430*, 213648.
[15] A. Brzechwa-Chodzyńska, W. Drożdż, J. Harrowfield, A. R. Stefankiewicz, *Coord. Chem. Rev.* **2021**, *434*, 213820.
[16] F. Würthner, A. Sautter, *Org. Biomol. Chem.* **2002**, *1*, 240–243.
[17] P.-P. Jia, Y.-X. Hu, Z.-Y. Peng, B. Song, Z.-Y. Zeng, Q.-H. Ling, X. Zhao, L. Xu, H.-B. Yang, *Inorg. Chem.* **2022**, *62*, 1950–1957.
[18] S. Pullen, S. Löffler, A. Platzek, J. J. Holstein, G. H. Clever, *Dalton Trans.* **2020**, *49*, 9404–9410.
[19] C. Colomban, C. Fuertes-Espinosa, S. Goeb, M. Sallé, M. Costas, L. Blancafort, X. Ribas, *Chem. Eur. J.* **2018**, *24*, 4371–4381.
[20] M. S. Deshmukh, V. S. Mane, A. S. Kumbhar, R. Boomishankar, *Inorg. Chem.* **2017**, *56*, 13286–13292.
[21] A. J. Plajer, E. G. Percástegui, M. Santella, F. J. Rizzuto, Q. Gan, B. W. Laursen, J. R. Nitschke, *Angew. Chem. Int. Ed.* **2019**, *58*, 4200–4204.
[22] R. Li, M. Han, J. Tessarolo, J. J. Holstein, J. Lübben, B. Dittrich, C. Volkmann, M. Finze, C. Jenne, G. H. Clever, *ChemPhotoChem* **2019**, *3*, 378–383.
[23] M. Han, R. Michel, B. He, Y. Chen, D. Stalke, M. John, G. H. Clever, *Angew. Chem. Int. Ed.* **2013**, *52*, 1319–1323.
[24] P. D. Frischmann, V. Kunz, F. Würthner, *Angew. Chem. Int. Ed.* **2015**, *54*, 7285–7289.
[25] S. Anderson, H. L. Anderson, A. Bashall, M. McPartlin, J. K. M. Sanders, *Angew. Chem. Int. Ed.* **1995**, *34*, 1096–1099.

[26] J.-L. Zhu, L. Xu, Y.-Y. Ren, Y. Zhang, X. Liu, G.-Q. Yin, B. Sun, X. Cao, Z. Chen, X.-L. Zhao, H. Tan, J. Chen, X. Li, H.-B. Yang, *Nat. Commun.* **2019**, *10*, 4285.
[27] F. Würthner, A. Sautter, D. Schmid, P. J. A. Weber, *Chem. Eur. J.* **2001**, *7*, 894–902.
[28] Z. Li, N. Kishi, K. Yoza, M. Akita, M. Yoshizawa, *Chem. Eur. J.* **2012**, *18*, 8358–8365.
[29] A. Walther, I. Regeni, J. J. Holstein, G. H. Clever, *J. Am. Chem. Soc.* **2023**, *145*, 25365–25371.
[30] I. Regeni, R. Chowdhury, K. Terlinden, S. Horiuchi, J. J. Holstein, S. Feldmann, G. H. Clever, *Angew. Chem. Int. Ed.* **2023**, *62*, e202308288.
[31] M. Käseborn, J. J. Holstein, G. H. Clever, A. Lützen, *Angew. Chem. Int. Ed.* **2018**, *57*, 12171–12175.
[32] N. A. Romero, D. A. Nicewicz, *Chem. Rev.* **2016**, *116*, 10075–10166.
[33] A. J. C. Kuehne, M. C. Gather, *Chem. Rev.* **2016**, *116*, 12823–12864.
[34] R. Coico, *Curr. Protoc. Microbiol.* **2006**, *00*, A.3 C.1–A.3 C.2.
[35] S. Wang, B. Li, F. Zhang, *ACS Central Sci.* **2020**, *6*, 1302–1316.
[36] I. Regeni, B. Chen, M. Frank, A. Baksi, J. J. Holstein, G. H. Clever, *Angew. Chem. Int. Ed.* **2021**, *60*, 5673–5678.
[37] H. Duan, T. Yang, Q. Li, F. Cao, P. Wang, L. Cao, *Chin. Chem. Lett.* **2024**, *35*, 108878.
[38] E. G. Percástegui, T. K. Ronson, J. R. Nitschke, *Chem. Rev.* **2020**, *120*, 13480–13544.
[39] T. Sawada, M. Yoshizawa, S. Sato, M. Fujita, *Nat. Chem.* **2009**, *1*, 53–56.
[40] A. M. Agafontsev, A. Ravi, T. A. Shumilova, A. S. Oshchepkov, E. A. Kataev, *Chem. A Eur. J.* **2019**, *25*, 2684–2694.
[41] E. A. Kataev, T. A. Shumilova, B. Fiedler, T. Anacker, J. Friedrich, *J. Org. Chem.* **2016**, *81*, 6505–6514.
[42] S. H. Hewitt, G. Macey, R. Mailhot, M. R. J. Elsegood, F. Duarte, A. M. Kenwright, S. J. Butler, *Chem. Sci.* **2020**, *11*, 3619–3628.
[43] J. Oh, H.-W. Rhee, J.-I. Hong, in *Synthetic Receptors for Biomolecules: Design Principles and Applications*, The Royal Society of Chemistry, Cambridge **2015**.
[44] S. Saha, I. Regeni, G. H. Clever, *Coord. Chem. Rev.* **2018**, *374*, 1–14.
[45] A. Jerschow, N. Müller, *J. Magnetic. Reson.* **1996**, *123*, 222–225.
[46] A. Jerschow, N. Müller, *J. Magn. Reson.* **1998**, *132*, 13–18.
[47] N. Puri, E. Zamaratski, C. Sund, J. Chattopadhyaya, *Tetrahedron* **1997**, *53*, 10409–10432.
[48] O. Plietzsch, A. Schade, A. Hafner, J. Huuskonen, K. Rissanen, M. Nieger, T. Muller, S. Bräse, *Eur. J. Org. Chem.* **2013**, *2013*, 283–299.

Manuscript received: October 3, 2024
Accepted manuscript online: October 29, 2024
Version of record online: November 19, 2024